HYBRIDIZATION OF HETEROGENEOUS 3D CFD DISCRETIZATIONS VIA DIRECT FLUX OPTIMIZATION

Boris Epstein , Sergey Peigin*
The Academic College of Tel-Aviv Yaffo, *Israel Aerospace Industries

Keywords: *Heterogeneous discretization, High order scheme, Non-point-to-point matched grids,Navier-Stokes computations*

Abstract

The paper handles the problem of accuracy loss of CFD solutions stemming from the use of computational domains with a heterogeneous discretization within the sub-domains. The problem occurs, e.g. where high-order numerical schemes are tailored with low order schemes, or where the same order approximations are applied to blocks with different grid resolution. The problem is especially troublesome for high accuracy CFD solutions where tailoring of heterogeneous meshes frequently brings loss of accuracy on a global scale.

The paper focuces on the treatment of non-point-to-point (NPP) structured grids that is grids in which block boundaries are not necessarily point-matched. In the context of high accuracy characteristic finite-volume schemes for 3D Navier-Stokes equations, a new approach is proposed which allows to maintain numerical stability and to minimize the accuracy loss due to variable grid resolution.

In the proposed approach interboundary cell clusters are formed which contain boundary cells from the neighbouring blocks of different resolution. For each such cluster, the residuals of the Navier-Stokes equations are computed ("collection" stage) and, finally, the cluster residuals are distributed among the cells of the host cluster by directly minimizing the flux disbalance in an appropriate norm ("distribution" stage). Outside the boundary clusters, the residuals are computed in the regular way.

The method allows to automatically preserve flux conservativity by placing constraints upon the optimum, it does not change the stability properties of the basic ENO scheme and ensures sufficiently high level of approximation on grids with reduced resolution. The results which include a number of numerical tests for 2D and 3D wings indicate good accuracy and robustness of the method and its applicability to full-scale Navier-Stokes computations.

1 Introduction

The paper considers the problem of accuracy loss of CFD solutions on composite computational domains with a heterogeneous discretization within the sub-domains. The problem occurs, e.g. where high-order numerical schemes are tailored with low order schemes, or where the same order approximations are applied to blocks with different grid partition.

The problem is especially troublesome for implementation of high accuracy CFD solutions since 3D tailoring of heterogeneous discretizations frequently brings loss of accuracy not only locally but on a global scale.

Specifically we focus on the following case. Consider a structured multi-block computational grid around an aerodynamic configuration intended for the solution of full Navier-Stokes equations. Structured grids have important advantages which make them highly competitive

for practical CFD. They may provide high accuracy solutions without need in complicated data structures (such as linked lists or graphs) for their implementation, which make them suitable for high efficiency parallel computing [1]. Structured grids are also indispensable for CFD driven aerodynamic shape design since they allow for fast and consistent grid movement.

Structured grids are easy to compose of point-to-point (PP) matched blocks. Unfortunately, the use of PP grids for complex aircraft configurations becomes problematic due to the following reason. The nature of PP matching requires the propagation of the discrete topology of a block from aircraft surfaces to the outer boundaries of the grid ("computational infinity"). For complex aircraft configurations, the construction of such grids requires considerable human resources in terms of time and expertise. The regularity of the grids is frequently low, and the overall number of grid points becomes prohibitively high.

The above considerations brought a number of researchers, especially in industry, to the idea of using non-point-to-point (NPP) structured grids that is grids in which block boundaries are not necessarily point-matched (Ref. [6]-[10]). NPP grids may significantly facilitate use of structured grids, but the approach appeared somewhat flawed for the following reasons. Firstly, in order to ensure the conservativity of numerical fluxes, it is necessary to tailor neighbouring blocks with different cell partition. This usually requires the exact adjustment of neighbouring boundary block cells, located from both sides of the joint boundary. The corresponding grid-generating procedure becomes sophisticated in the three-dimensional case. The second class of problems is associated with the implementation of high accuracy characteristic numerical schemes like in [1]-[3] in the case where the neighboring blocks possess different grid resolution on the both sides of the joint boundary. To maintain a high-order discretization across the inter-block boundary, the current flow solution is usually interpolated which inevitably introduces high amounts of artificial dissipation and may severely affect the accuracy of computations.

Within the framework of a time-iterated finite-volumes scheme of [2] in this work we propose a new approach to the problem of NPP. In the vicinity of each NPP inter-block boundary, we form time-independent auxiliary clusters of minimum volume in such a way that 1) each cluster contains boundary cells from the neighbouring blocks of different resolution 2) the cluster boundary is composed of cell faces which belong to only one of the neighbouring blocks. Thus the original inter-block boundary is "swallowed" by the cluster. In each time step, the residual computation is done in three stages. In the first stage, the residuals are calculated at the "non-boundary" (regular) numerical cells, i.e. at the cells which do not belong to any of the above described clusters. Note that such cells constitute the vast majority of cells. The calculation is performed in a regular way as if the grid was of PP type (specifically, by means of the ENO flux interpolating scheme, see [2] and Section 2 of the present paper). In these cells, no information "across the block boundary" is needed for the residual calculation, so the block localized numerical procedure is not affected by the distinction in grid resolution between the neighbouring blocks.

It is important that already in the course of the first stage, numerical fluxes were also determined at the outer boundary of the above clusters since this boundary is composed of faces of the regular cells. In the second ("collection") stage, the cluster residuals are computed. This is feasible since the numerical fluxes at the cluster boundary, are available from the first-stage computation stage as just explained in the previous paragraph. The overall cluster flux balance is thus composed of the fluxes at the cell faces which constitute the cluster boundary.

In the last, third ("distribution") stage, the residuals at the "irregular" cells which belong to one of the clusters, are determined by minimizing algebraically the flux disbalance in an appropriate norm. Note that the optimization is performed for each cluster separately, and thus the number of optimization parameters is low. After the third stage, the residuals are calculated at all numerical cells of the composed grid, and the solution is

advanced "in time" by the usual time integrating procedure.

The method allows to automatically preserve the conservativity of the numerical scheme by placing simple constraints upon the optimization process. As a result, the cell tailoring procedure usually typical of NPP schemes became redundant. The hybrid calculation of residuals did not change the stability properties of the basic ENO numerical scheme, and ensured sufficiently high level of accuracy on actually less resolved grids. The time expenditure for the residual handling at "irregular" cells (Stages 2 and 3) appeared negligible and did not harm the high parallelization efficiency of the method. The results which include a number of numerical tests for two-and three dimensional wings indicate accuracy and robustness of the method and its applicability to full-scale Navier-Stokes computations in engineering environment.

2 Preliminary Considerations

2.1 Basic Numerical Approach

We start with a finite-volume numerical ENO scheme developed in Ref.[2]- [3] for the solution of steady-state Navier-Stokes equations on point-to-point matched structured multiblock grids. In Cartesian coordinates the continious equations take the form:

$$\frac{\partial \mathbf{q}}{\partial t} + \mathrm{div}\mathbf{C} = \mathrm{div}\mathbf{V} \qquad (1)$$

where the tensor $\mathbf{C} = (\mathbf{f}, \mathbf{g}, \mathbf{h})$ represents the convection terms, the tensor $\mathbf{V} = (\mathbf{r}, \mathbf{s}, \mathbf{t})$ represents the viscous terms, $\mathbf{q} = (\rho, \rho\mathbf{u}, \rho\mathbf{v}, \rho\mathbf{w}, E)$, ρ is the density, $(\mathbf{u}, \mathbf{v}, \mathbf{w})$ is the velocity vector, E is the energy, t is the time, $\mathbf{f}, \mathbf{g}, \mathbf{h}$ are the inviscid (convection) fluxes and $\mathbf{r}, \mathbf{s}, \mathbf{t}$ are the viscous fluxes which depend in a nonlinear mode on $\mathbf{q}$.

The above assumption of PP matched structured blocks means that the grid consists of a number of blocks, where each block has (i, j, k) structure and that interblock boundaries are point-to-point matched (see Fig. 1).

Integrating over each cell separately in a finite-volime manner, we get a system of ODE's which can be solved by a time-stepping procedure. For particular cell (i, j, k) the following approximation is assumed:

$$\begin{aligned}
&(\Omega_{i,j,k}\mathbf{q}_{i,j,k})_t + [\mathbf{C}\cdot(S\mathbf{n})]_{i+0.5,j,k} \qquad (2)\\
&-[\mathbf{C}\cdot(S\mathbf{n})]_{i-0.5,j,k} + [\mathbf{C}\cdot(S\mathbf{n})]_{i,j+0.5,k}\\
&-[\mathbf{C}\cdot(S\mathbf{n})]_{i,j-0.5,k} + [\mathbf{C}\cdot(S\mathbf{n})]_{i,j,k+0.5}\\
&-[\mathbf{C}\cdot(S\mathbf{n})]_{i,j,k-0.5} = [\mathbf{V}\cdot(S\mathbf{n})]_{i+0.5,j,k}\\
&-[\mathbf{V}\cdot(S\mathbf{n})]_{i-0.5,j,k} + [\mathbf{V}\cdot(S\mathbf{n})]_{i,j+0.5,k}\\
&-[\mathbf{V}\cdot(S\mathbf{n})]_{i,j-0.5,k} + [\mathbf{V}\cdot(S\mathbf{n})]_{i,j,k+0.5}\\
&-[\mathbf{V}\cdot(S\mathbf{n})]_{i,j,k-0.5}
\end{aligned}$$

where $\Omega_{i,j,k}$ is the cell volume, $\mathbf{q}_{i,j,k}$ in some mean value of $\mathbf{q}$ over the cell and S is the area of a cell side surface.

Fluxes with half-indices are approximated by a one-dimensional interpolation from the near-by cell centers, based on the ENO concept (Ref. [4]) with a specific flux interpolation technique close to that of Ref. [5].

Non-linear stability is maintained via approximation of inviscid fluxes on a variable template according to local characteristics and smoothness of the fluxes; viscous fluxes are approximated in a straightforward way. An ENO interpolation template (typically consisting of 3 points on the finest multigrid level) is determined separately for each characteristic field, primarily according to the sign of the corresponding eigenvalue, and then according to the smoothness of fluxes.

In the framework of the method, the above mentioned ENO procedure is applied only for the defect correction calculation, a very limited number of times (roughly equal to the number of multigrid cycles), and most of the computational work is performed using a relatively cheap upwind biased relaxation.

A 3 stage Runge-Kutta scheme is used in a Total Variation Diminishing (TVD) form [5]. Specially constructed algorithms are used to diminish considerably the amount of computational work associated with changeability of template.

Note that the conservativity of the scheme was achieved through the transparency of interblock boundaries in such a way that the interpolation template might include the cell values across the block boundary.

2.2 Discussion of the Problem

In this work we aim to extend the above numerical scheme of [1]-[3] to non-point-to-point matched meshes. In this case, numerous problems arise even within of low-order numerical schemes or incompressible flows. Within a more demanding framework of high-order characteristic schemes on NPP grids, the following interrelated numerical drawbacks must be overcome: loss of accuracy, deterioration of stability and violation of conservativity. To illustrate this consider a fragment of a model 2D NPP grid depicted in Fig. 2 , where Block 2 possesses a twice higher partition in y direction tnan Block 1 while keeping the same as in Block 1 partition in x direction,

First, consider the Poisson equation:

$$\Delta u = 0 \tag{3}$$

which models viscous terms in full Navier-Stokes equations. Looking for the finite-volume solution on the grid of Fig. 2, we must approximate the term $u_x \cdot |AB|$, which is the numerical flux at the face AB, located at the boundary between Block1 and Block 2. A natural approximation for this is the finite difference $(u_D - u_C)/h_x$. Since Block 2 is twice finer in y direction it does not provide the value u at point D but instead two values above and below D: D^{up} and D^{low} are available. The linear interpolation based these values yields the following approximation

$$u_x = \frac{0.5(u_D^{up} + u_D^{low}) - u_C}{h_x}$$

This means that the order of approhimation of Poisson equation at point C is

$$\frac{u_E - 2u_C + 0.5(u_D^{up} + u_D^{low})}{h_x^2} + \tag{4}$$

$$+ \frac{u_F - 2u_C + u_G}{h_y^2} = O(h_x^2 + h_y^2) + O\left(\frac{h_y^2}{h_x^2}\right)$$

It is possible to improve the order of approximation in this model case by enlarging the computational template in x direction or by significantly increasing the order of interpolation in the y direction. Note that in the both cases, the approximation to the equation is not even consistent where $h_y >> h_x$.

Now consider the approximation of convective terms of Eq.(1) on the grid of Fig. 2. At the face AB which belongs in Block 1, ENO template for the interpolation of characteristic fluxes may include point D even in the case of a low-order approximation. Similar to the approximation of viscous terms, the needed solution value at this point must be interpolated using the actually existing grid points D^{up} and D^{low} of Block 2. Similar to relation (4), a straightforward interpolation yields the order of approximation greater or equal to $O(h_y^2/h_x)$, which is again prohibitive where $h_y >> h_x$.

In the approximation of inviscid terms, an additional serious problem arises since the above interpolation may be antidissipative leading to numerical instability. As the order of non-characteristic interpolation increases, prompted by the requirement of accurate approximation, the enhancement of stability becomes even more conjectural.

This means that in order to ensure the stability and accuracy of the method, a high order characteristic interpolation of the solution is needed, in the direction orthogonal to this of the flux interpolation. This highly complicates the basic numerical scheme and actually eliminates the advantages of one-dimensional flux interpolation of Ref. [3], [5] on structured grids.

The third problem is that of preserving the conservativity properties of the numerical scheme. E.g., a flux at face AB calculated at cell C must be equal to the sum of the corresponding face fluxes calculated at cells D^{up} and D^{low}. This requires not only the full geometrical conformity of the boundary faces from both sides of the interblock boundary, but also the exact adjustment of the corresponding numerical fluxes.

Remind that the numerical procedure of Ref. [3], [5] performs flux interpolation in the charac-

teristic fields. Thus the adjustment of numerical fluxes implies the adjustment the corresponding eigen values on the both sides of the boundary. These are non trivial requirements even for a simple grid of Fig. 2. For curvilinear 3D NPP structured blocks with arbitrary partition, the solution of the problem becomes almost infeasible.

3 New Approach

Based on the considerations of the previous section we observe that the approximation of NPP block boundary fluxes is troublesome in terms of accuracy and stability. This may lead to intractable problems and seriously flaw the use of NPP structured grids.

On the other hand the problem is confined to narrow strips in the vicinity of NPP block boundaries. This gives rise to the following idea. Block boundary fluxes are only needed in order to determine residuals in the bordeline cells. These residuals may be computed through an alternative numeric procedure different from the basic ENO technique. The both numerical procedures must be of course compatible in order to ensure the conservativity of the resulting composite scheme.

Before describing the new procedure in details, the following remark may be made. In principle, it is possible to numerically solve boundary-value problem for a partial differential equation by directly minimizing the residuals of a discrete approximation in an appropriate norm. Some attempts in this direction have been made in the recent years in the field of CFD. So far, these attempts were confined to low-accuracy gas-dynamic models on relatively coarse grids. In our opinion, the reason for this lies in the fact that optimization methods become highly inefficient where high-dimensional search spaces are needed, which is the case where Euler or Navier-Stokes equations are to be solved. E.g. for a relatively simple geometry of 3D aerodynamic wing, the number of optimization parameters (flow-field variables) may reach several hundred thousands or even one million which makes existing optimization methods practically non-applicable.

An additional dificulty related to this approach is illustrated by the following example. Consider Burgers' equation

$$\frac{\partial}{\partial x}\left(u^2\right) = 0, \quad u(-\infty) = 1, \quad u(\infty) = -1 \quad (5)$$

and a simple finite-volume approximation to it at each cell i with center x_i:

$$Res_i = (u^2)_{i+1/2} - (u^2)_{i-1/2} = 0,$$

$$i = 0, \pm 1, \pm 2, \ldots \pm (N-1), \quad u_{-N} = 1, \quad u_N = -1$$

The solution is being sought at the centers of cells $\{x_i\}$ while the specific numerical scheme is determined by an interpolation of fluxes $f_i = u^2$ from $\{x_i\}$ to $\{x_{i\pm 1/2}\}$.

Minimizing the L^2 residuals norm

$$\sum_i (Res_i)^2 = \sum (f_{i+1/2} - f_{i-1/2})^2, \quad f_{-N} = f_N = 1$$

we come to the trivial solution $f_{k+1/2}$=1 for all k, which does not provide sufficient information on the solution $\{u_i\}$. For example, any consistent flux interpolation $I : \{f_i\} \to \{f_{i+1/2}\}$ and any solution $\{u_i\}$ representing the permutation of 1 and -1 yield $\{f_i\} = 1$ and, consequently $\{f_{i+1/2}\} = 1$.

The situation changes where direct residual minimization is restricted to a small subdomain of the computational grid such as interblock strips or their subsets. In this case the number of optimization parameters is relatively low which makes the optimization practically feasible. On the other hand, the compatibility of the optimization procedure with the characteristic flux determination on the boundary of the subdomain, does not allow for saw-tooth solutions.

The proposed algorithm for residual determination in the boundary interblock strips includes several stages.

In the preliminary ("preprocessing stage") time-independent auxiliary cell clusters are formed. Each such cluster comprises cells of the existing grid taken from the neighbouring blocks of different partition in such a way that the following two properties are fulfilled:

- Property 1: the cluster boundary is composed of cell faces which do not belong to the interblock boundary
- Property 2: each cluster represents a "minimum volume" set, that is its own cell subclusters do not satisfy Property 1

For example, in Fig. 2, cells C (Block 1), D^{up} and D^{low} (Block 2) comprise such a cluster since A) the boundary of the cluster includes three faces of cell C ("west", "north" and "south"), 2 faces of cell D^{up} ("north" and "east") and 2 faces of cell D^{low} ("south" and "east"), each belonging to only one of the blocks and B) any cell deletion from this cluster will destroy the "single citizenship" Property 1.

Finally, the above cluster definitions imply that the original interblock boundary is "swallowed" by the cluster. E.g., in Fig. 2, the interblock face AB became internal to the cluster $\{C, D^{up}, D^{low}\}$.

Thus the preprocessing stage performs the minimal cluster covering of those grid cells which 1) possess a cell face which belong to two neighbouring blocks; 2) the above two blocks possess a diferent resolution in a direction tangential to the interblock boundary surface.

At each iteration, the computation of residuals is divided into three stages.

In the first stage of the numerical procedure, the residuals are determined in the "regular" cells that are cells which do not belong to the above cluster covering. The calculation is performed by means of a regular ENO flux interpolating scheme described in Section 2.1.

This calculation, similar to that for point-to-point matched grids, is feasible, since in the "regular" cells, it is possible to perform a characteristic flux interpolation without necessaraly using the information from other side of the interblock boundary. For example, in terms of Fig. 2, the flux at the "west" face of cell C has at hand not only the solution values at cell centers to the west of the face but also the values at C which is sufficient for stability of the numerical process.

Of course, "regular" cells constitute the vast majority of grid cells. It is important for the following, that in the course of the first stage, the numerical fluxes have been determined at all boundaries of the clusters (built at the prepocessing stage), since the boundaries are formed by faces of the regular cells.

This allows to perform the second stage of the numerical procedure - the "collection" stage, where "cluster residuals" are determined. More exactly, the overall flux balance of a cluster is composed of the fluxes at the faces of the cluster boundary. As just explained above, the fluxes at the cluster boundary have been calculated at the first ("regular") stage since they also belong to the regular cells.

In the third ("distribution") stage, it is necessary for each cluster to distribute the cluster residuals between the cells which make it up. Remind, that the cell flux balance represents (within a factor of volume) the residual of the steady-state equation. Thus the minimization of cell residuals is equivalent to the minimization of cell flux balances in an appropriate norm.

This is performed algebraically subject to the following constraints: A) The overall cluster flux balances are equal to those computed at the collection stage; B) The flux conservativity of the numerical scheme is preserved. The last property is satisfied by placing simple constraints upon the optimization procedure.

The optimization proceeds separately for each cluster which keeps the number of optimization parameters to a low level. After the third stage, the residuals are determined in all the grid cells which allows to advance the solution by the usual time-stepping scheme of Section 2.1.

Going back to Poisson equation (3) a simple check shows that the new procedure ensures (contrary to the "naive" scheme) an order of approximation of $O(h_x^2 + h_y^2)$. First, the exact solution of the Poisson equation satisfies the finite-volume expression for the cluster residual within an error of $O(h_x^2 + h_y^2)$. The same is true for the "distributed" cell residuals since they are minimized subject to the preservation of the overall cluster residual.

This illustrates that the new procedure provides a natural mechanism for accurate approxi-

mation at non-mathched block boundaries.

Since the composite numerical procedure fully preserves the conservativity of the scheme, NPP block tailoring procedure which is typically employed with this end of view, becomes redundant.

It appeared that the hybrid residual calculation procedure does not have an adverse effect on the stability of the original ENO numerical scheme while the time expenditure for the treatment of "irregular" cells is negligible, which allows to retain the high parallel efficiency of the method. The proposed procedure allowed to minimize loss of accuracy due to the tailoring of NPP matched blocks and to prevent loss of accuracy on a large scale.

4 The Resulting Numerical Scheme

4.1 Generic Model Problem

Consider the numerical scheme stemming from the proposed approach for several simple but representative model problems. With thid end in view we introduce an one-dimensional grid consisting of cells of length h:

$$x_i = h \cdot (1 - 1/2)$$

where cell centers correspond to $i = 1,2,3,\ldots$ and cell boundaries are set at $i = 1/2, 3/2, 5/2, \ldots$. We are interested in the steady-state solution for a generic equation:

$$\frac{\partial u}{\partial t} + \frac{\partial f}{\partial x} = 0, \tag{6}$$

In the following we will consider the hyperbolic case where $f = f(u)$.

The model equation is solved by a finite-volume numerical scheme

$$\frac{\partial u_i}{\partial t} + \frac{f_{i+1/2} - f_{i-1/2}}{h} = 0, \tag{7}$$

starting from an initial guess

$$u^\circ = u(0,x) \tag{8}$$

with addition of appropriate boundary conditions.

To model the proposed approach we assume that the cell boundary at $i = k + 1/2$ represents a non-point-to-point face, that is the flux value at this face can not be computed by a regular way (through the values at the neghbouring cell centers), and, instead, is subject to the procedure described in the previous section. Our aim is to check the influence of the changes thus introduced into numerical scheme, on the stability of the method, and to formulate necessary consistency conditions.

4.2 Linear Wave Equation

Here, $f(u) = u$ and a simple upwind scheme

$$\frac{\partial u_i}{\partial t} + \frac{u_i - u_{i-1}}{h} = 0, \tag{9}$$

which corresponds to the approximation $f_{i+1/2} = u_i$ is a stable TVD-type scheme on the regular grid (where $i = k + 1/2$ is not singled out) under appropriate CFL conditions.

Within the present approach a non-matching face $x_{k+1/2}$ and the trivial residual optimization at the adjacent cells k and $k+1$, the scheme at these cells becomes:

$$\frac{\partial u_k}{\partial t} + R = 0, \quad \frac{\partial u_{k+1}}{\partial t} + R = 0, \quad R = \frac{u_{k+1} - u_k}{2h}, \tag{10}$$

while at the remaining ("regular") cells the scheme remains unchanged. The new composite scheme is again of TVD-type at $x = x_{k+1}$ and at all the regular cells as well. Since the value of the numerical solution at $x = x_k$ does not influence the solution at other points, this is quite acceptable. In fact, since due to (10)

$$\frac{\partial (u_k - u_{k+1})}{\partial t} = 0$$

for each t (at all iteration steps), then

$$u_k - u_{k+1} = u_k^\circ - u_{k+1}^\circ$$

irrespective of t.

This means, that in order to satisfy the approximation properties of the scheme at $x = x_k$, the initial guess must be chosen in a consistent way.

4.3 Non-linear 1-D Conservation Law

Now we consider a more challenging case of the steady-state solution for a non-linear equation (6), where $f = f(u)$ depends non-linearly on u. A good example for this is the Burgers' equation:

$$f = \frac{1}{2}u^2, \quad u(0) = 1, \quad u(1) = -1,$$

again solved on the generic grid of Section 4.1 with a "non-matched" grid singularity at $x = x_k$.

Consider a simple upwind flux approximation with entropy fix:

$$f_{i+1/2} = f_i, \quad if \quad f'(u_i) > 0, \quad f'(u_{i+1}) > 0$$
$$f_{i+1/2} = f_{i+1}, \quad if \quad f'(u_i) < 0, \quad f'(u_{i+1}) < 0 \tag{11}$$

and

$$f_{i+1/2} = \frac{1}{2}(f^+_{i+1/2} + f^-_{i-1/2}), \quad f^+_{i+1/2} = f_i + \lambda u_i,$$
$$f^-_{i+1/2} = f_{i+1} - \lambda u_{i+1},$$
$$\lambda = max\{|f'(u_i)|, |f'(u_{i+1})|\}$$

in the remaining cases.

Similar to (9)-(10), the scheme changes at points k, $k+1$ with

$$R = \frac{f_{k+3/2} - f_{k-1/2}}{2h},$$

where $f_{k+3/2}$ and $f_{k-3/2}$ are chosen according to (11).

If sign of $f'(u)$ does not change at faces $k-1/2$, $k+1/2$ and $k+3/2$, the scheme retains its TVD properties in the same way as explained in the previous section. E.g., if $f'(u) > 0$ at these points, $f_{k+3/2} = f_{k+1}$, $f_{k-1/2} = f_{k-1}$, and similar to the above described, the scheme is of TVD type at the regular points ($i \neq k$, $i \neq k+1$) and at $i = k+1$ under appropriate CFL conditions. Similar to the example of Section 4.1, the solution at $i = k$ does not influence the solution at other points but for consistency the initial guess at $i = k$ and $i = k+1$ must be compatible.

Now consider two more challenging situations. First, consider the case where the non-matching face at $i = k+1/2$ lies just to the right of the current shock position, that is $f'(u_i) > 0$ for $i \leq k-1$ and $f'(u_i) < 0$ for $i \geq k$. Then the regular scheme changes at cell $k-1$, k and $k+1$. With $\lambda = max\{|f'(u_{k-1})|, |f'(u_k)|, |f'(u_{k+1})|\}$ we have the following relations.

A. For case $i = k-1$, the residual is determined as follows:

$$R = \frac{T}{2h}, \quad T = f_{k-1/2} - f_{k-3/2} =$$
$$= \frac{1}{2}[f_{k-1} + \lambda u_{k-1} + f_k - \lambda u_k] - f_{k-2} =$$
$$= \frac{1}{2}[f_k - f_{k-1} + 2(f_{k-1} - f_{k-2}) + \lambda(u_{k-1} - u_k)] =$$
$$= \frac{1}{2}[(u_{k-1} - u_k)(\lambda - f'(u^*)) +$$
$$+ 2f'(u^{**})(u_{k-1} - u_{k-2})]$$

where $u^* = u(x^*)$, $u^{**} = u(x^{**})$, $x^* \in (x_{k-1}, x_k)$, $x^{**} \in (x_{k-2}, x_{k-1})$, and thus $f'(u^{**}) > 0$. If, e.g., $u_{k-1} \geq max\{u_k, u_{k-2}\}$, then $T > 0$ and, consequently the value of u_{k-1} will be decreased by the iteration, and, similarly, the value of u_{k-1} will be increased by the iteration where $u_{k-1} \leq min\{u_k, u_{k-2}\}$.

B. For case $i = k$, the residual is determined as follows:

$$R = \frac{T}{2h}, \quad T = f_{k+3/2} - f_{k-1/2} =$$
$$= f_{k+2} - \frac{1}{2}[f_{k-1} + \lambda u_{k-1} + f_k - \lambda u_k] =$$
$$= \frac{1}{2}[2(f_{k+2} - f_k) + f_k - f_{k-1} + \lambda(u_k - u_{k-1})] =$$
$$= \frac{1}{2}[2f'(u^*)(u_{k+2} - u_k) + (u_k - u_{k-1})(\lambda + f'(u^{**})]$$

where $x^* \in (x_k, x_{k+2})$, $x^{**} \in (x_{k-1}, x_k)$. If, $u_k \geq max\{u_{k-1}, u_{k+2}\}$, then both terms in T are positive which leads to the decrease in the value of the local maximum u_k, with the adverse effect in the case of local minimum $u_k \leq min\{u_{k-1}, u_{k+2}\}$.

Here we exclude u_{k+1} from the consideration since this value does not influence the solution at other points. Similar to the previously described cases, the initial value u°_{k+1} must be compatible with u°_k in terms of approximation.

The second situation occurs where the sign of $f'(u)$ changes exactly across the non-matched face $i = k+1/2$, that is $f'(u_k)\cdot f'(u_{k+1}) < 0$. Note, that this may be avoided by setting $u^\circ_{k+1} = u^\circ_k$ since then

$$\frac{\partial u_k}{\partial t} = \frac{\partial u_{k+1}}{\partial t}$$

and $u_{k+1} = u_k$ at any time step. This, however, results in $O(h)$ accuracy in the vicinity of the non-matched boundary.

With $u^\circ_{k+1} \neq u^\circ_k$ the situation is possible, where both the values u_{k+1} and u_k do not influence the numerical solution at other grid points which may disrupt the calculation on each side of the non-matched boundary. To avoid this we define

$$\lambda = max\{|f'(u_{k-1})|, |f'(u_k)|, |f'(u_{k+1})|, |f'(u_{k+2})|\}$$

and apply the entropy fix procedure at faces $k-1/2$ and $k+3/2$. Specifically, the value of residual multiplied by $2h$ becomes at $i = k$ and $i = k+1$ as follows:

$$\begin{aligned} T = \frac{1}{2}[f_{k+1} + f_{k+2} + \lambda(u_{k+1} - u_{k+2}) - \\ - f_{k-1} - f_k - \lambda(u_{k-1} - u_k)] = \\ = \frac{1}{2}[(\lambda + f'(u^*)(u_{k+1} - u_{k-1}) + \\ + (\lambda - f'(u^{**})(u_k - u_{k+2})] \end{aligned}$$

where $x^* \in (x_{k-1}, x_{k+1})$, $x^{**} \in (x_k, x_{k+2})$. Let us now assume, that a "true maximum" exists at the cells of the non-matched boundary if

$$min\{u_k, u_{k+1}\} \geq max\{u_{k-1}, u_{k+2}\}$$

Then T is positive which means that u_k and u_{k+1} are decreased. In the opposite case

$$max\{u_k, u_{k+1}\} \leq min\{u_{k-1}, u_{k+2}\}$$

u_k and u_{k+1} are increased. In this sense, the scheme retains its TVD properties.

The situation where a local minimum in k coexists with a local maximum in $k+1$ does not lead to the change in the total variation due to the condition

$$\frac{\partial u_k}{\partial t} = \frac{\partial u_{k+1}}{\partial t}$$

A more sophisticated case $u_k < u_{k-1} < u_{k+1} < u_{k+2}$ does not necessaraly increase the value of u_k. This is not dangerous in terms of stability since the variation $|u_{k-1} - u_{k+1}| + |u_{k+1} - u_{k+1}|$ does not change, and $|u_k - u_{k+1}| = |u^\circ_k - u^\circ_{k+1}|$.

Summing up, the modified scheme retains TVD properties in the above described sense, and at the expense of $O(h)$ in accuracy, is fully TVD.

5 Results and Discussion

To verify the proposed new approach, the above procedure was applied to the computation of the flow over RAE2822 airfoil at transonic conditions ($M = 0.75$). The original point-to-point matched grid comprised 4 blocks: upper airfoil, lower airfoil (with dimensions $i = 128$, $j = 96$ in the streamwise and normal directions, respectively) and upper wake and lower wake (with the corresponding dimensions $i = 64$, $j = 96$).

For the verification studies, the upper airfoil block was subdivided into 2 subblocks along the grid line $j = J^* = const$. A total of 3 test cases were considered (labeled as *Case_P*1 to *Case_P*3) for different values of the above constant. The dimensions of the first subblock (near the airfoil) was kept to the original level ($i = 128$, $j = J^*$), while the i-dimension of the second subblock was significantly reduced (from the original 128 to 64 and 48). The location of the cut line was varied in the wide range: from a remote (with respect to the airfoil) *Case_P*1 to a rather close *Case_P*3 where this line intersects the supersonic bell in the considered flight conditions.

The grid details can be found in Fig. 3-5, where iso-Mach contours for different test cases are presented. As it can be seen from these figures, the flow structure is basically independent of the location of the non-matched grid line.

As the whole the analysis of the results shows, that the new approach yields stable results with a negligible loss of accuracy. This conclusion can be illustrated by Fig. 6-8. In Fig. 6 we

see the comparison between C_P distributions for the original point-to-point computations vs. the most challenging case *Case_P*3. In terms of convergence, the proposed NPP tailoring approach produces results very similar to those of the original grid (see Fig. 7). Finally, Fig. 8 demonstrates, that the above described good accuracy of the proposed approach is preserved in a wide range of flight conditions.

5.1 Copyright Statement

References

[1] Peigin, S., Epstein, B., Rubin, T., and Seror, S., *Parallel large scale high accuracy Navier-Stokes computations on distributed memory clusters*, The Journal of Supercomputing, Vol. 27, 2004, pp.49–68.

[2] Epstein B, Averbuch A, Yavneh, I. *An accurate ENO driven multigrid method applied to 3D turbulent transonic flows*, J. Comput. Phys. Vol.168, 2001, pp.316–338.

[3] Epstein, B., Rubin, T., and Seror, S., *Accurate multiblock Navier-Stokes solver for complex aerodynamic configurations*, AIAA Journal, Vol. 41, No. 4, 2003, pp.582–594.

[4] Harten, A., Engquist, B., Osher, S., Chakravarthy, S., *Uniformly high order accurate non-oscillatory schemes. 1*, J. Comput. Phys, Vol. 71, 1987, pp.231–303.

[5] Shu. C.W., Osher, S., *Efficient implementation of essentially non-oscillatory shock-capturing schemes*, J. Comput. Phys. Vol.83, 1989, pp.32–78.

[6] Rai, M.M., *Conservative treatment of zonal boundaries for Euler equation calculations*, J. Comput. Phys. Vol.22, 1986, pp.472–503.

[7] Bohbot, J., Jouhaud. J.C., Darracq, D., *Coupled patched-grid AMR meshing techniques for transonic aircraft design*, AIAA Paper 2002-0546.

[8] Chen, H.X., Fu, S.J, *Navier-Stokes simulations for transport aircraft wing-body combinations with deployed high-lift systems*, AIAA Paper 2003-4077.

[9] Chen, S., Khalid, M., Zhang, S., *A non-continious grid generation method using ICEMCFD's HEXA*, Proc. of the 9th Annual Conference of CFD Society of Canada. Waterloo, Canada, May 27-29, 2001.

[10] Nataf, F., and Rogier, F., *Factorization of convective-diffusion operator and the Schwarz algorithm*, Math. Models and Methods in Appl. Sci., accepted for publication.

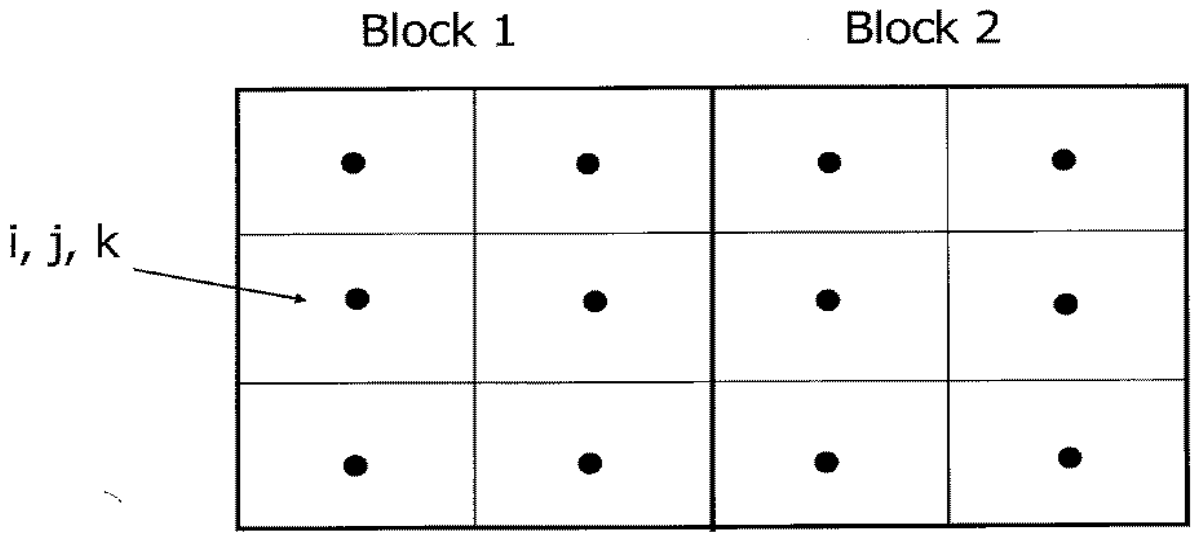

Fig. 1 Point-to-point matched structured grid.

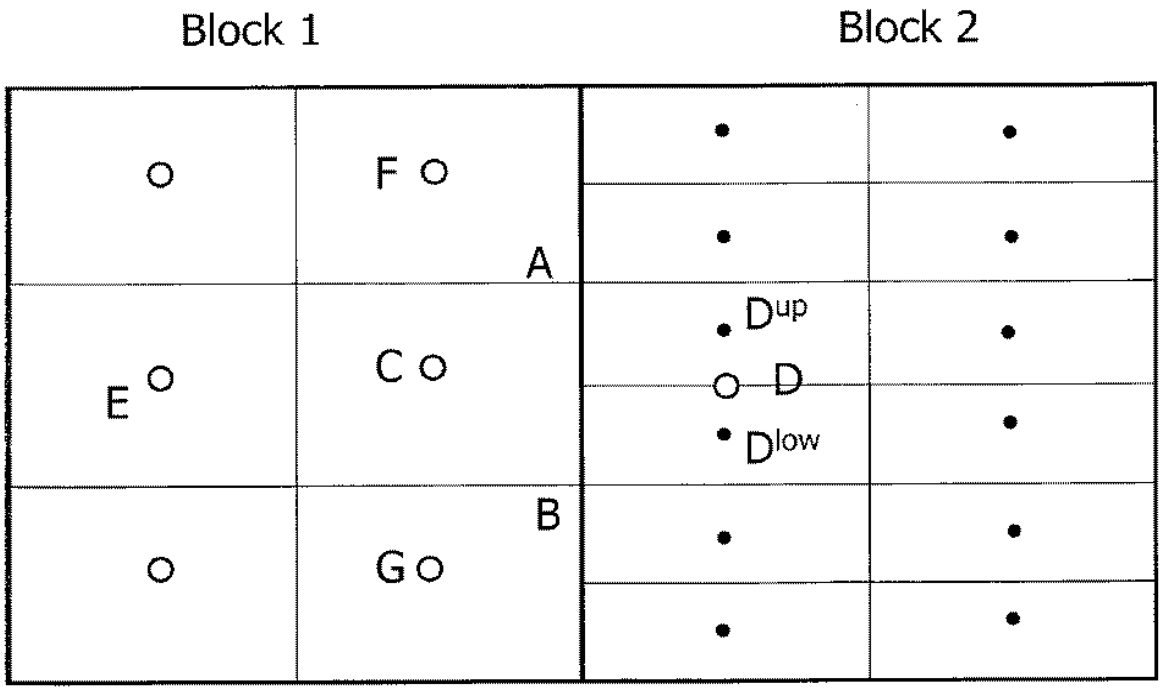

Fig. 2 Non-point-to-point matched structured grid.

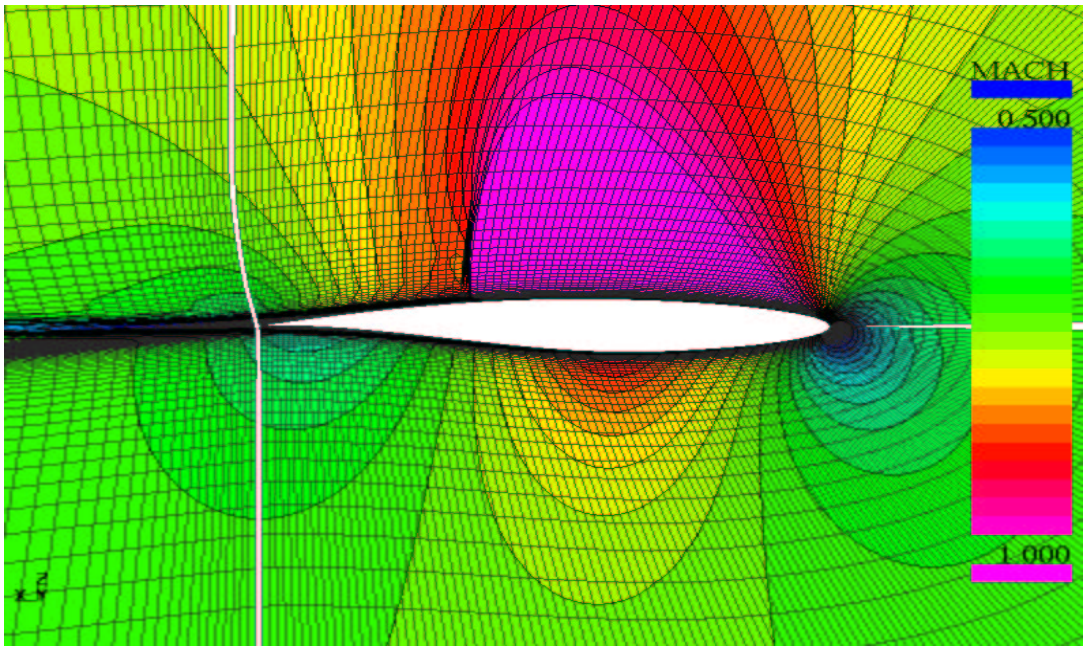

Fig. 3 Case_P1, NPP ratio 128:48. Iso-Mach contours at $\alpha = 1.5°$, $M = 0.75$.

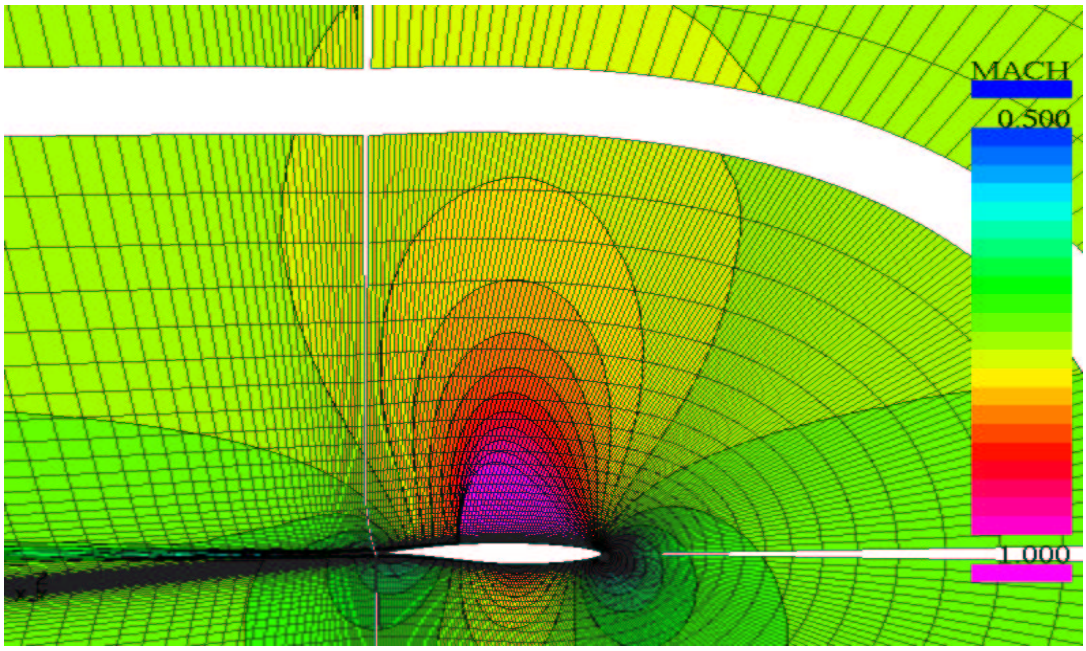

Fig. 4 Case_P2, NPP ratio 128:48. Iso-Mach contours at $\alpha = 1.5°$, $M = 0.75$.

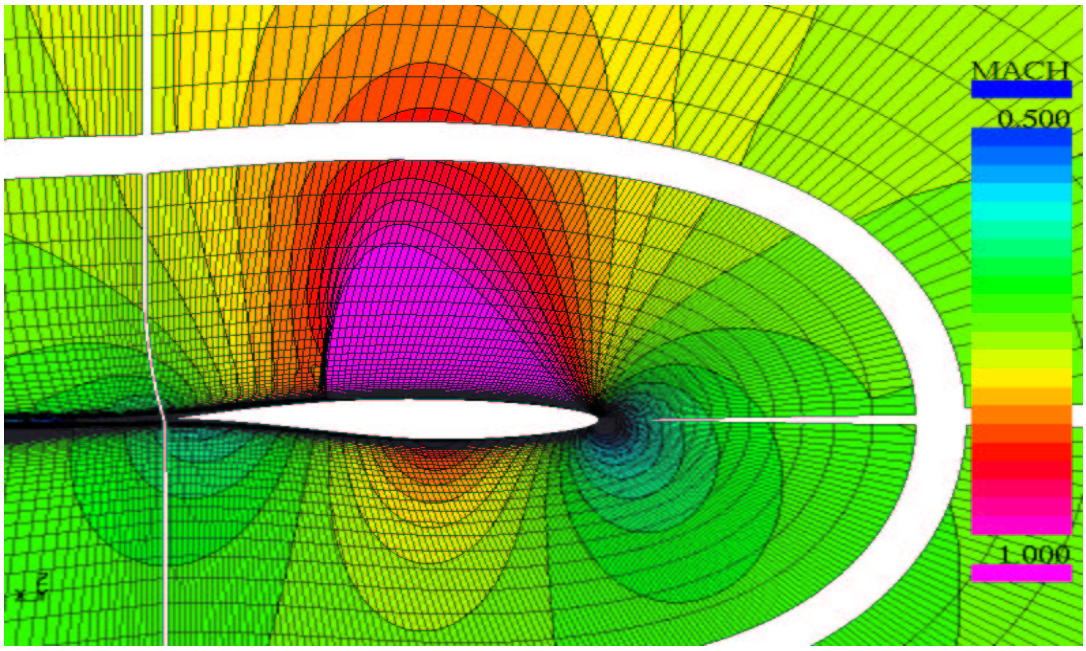

Fig. 5 Case_P3, NPP ratio 128:64. Iso-Mach contours at $\alpha = 1.5°$, $M = 0.75$.

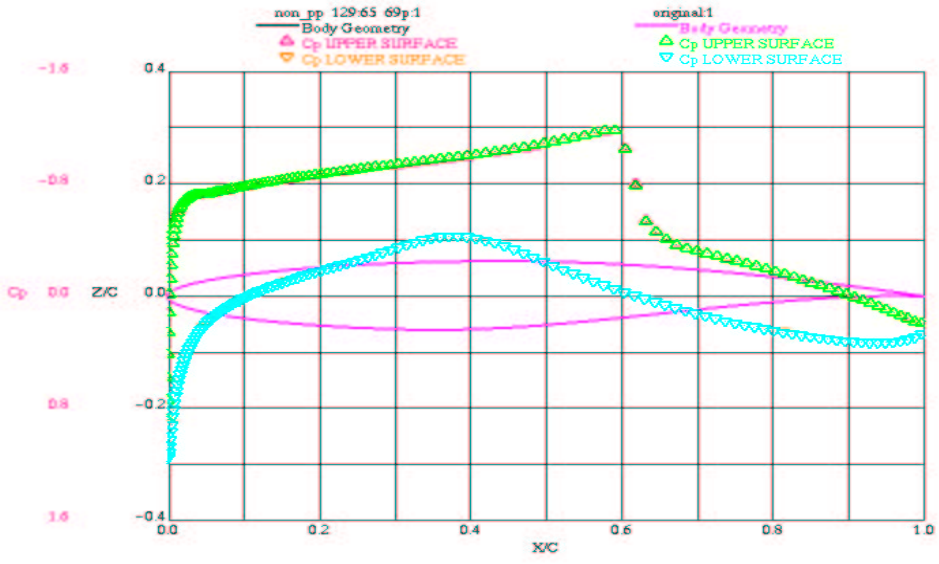

Fig. 6 Case_P3, NPP ratio 128:48. C_P distribution at $\alpha = 1.5°$, $M = 0.75$.

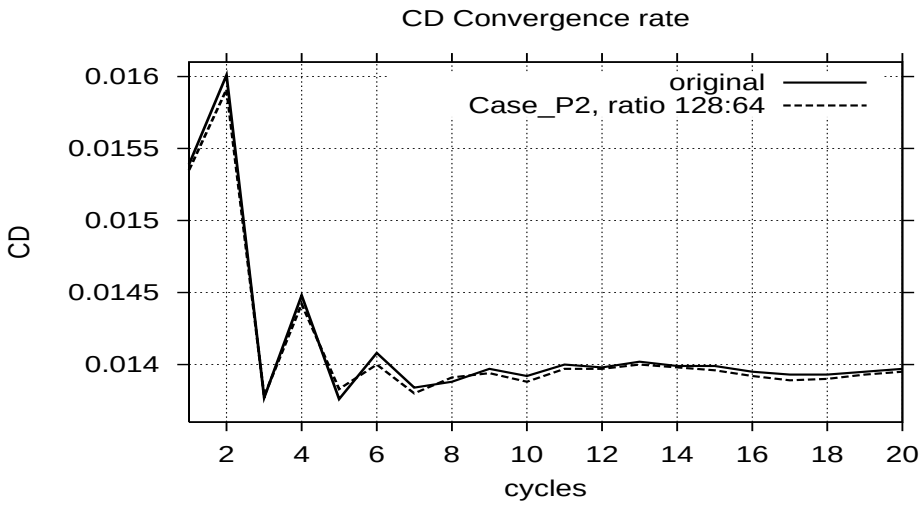

Fig. 7 Case_P2, NPP ratio 128:64. Convergence of C_D at $\alpha = 1.5°$, $M = 0.75$.

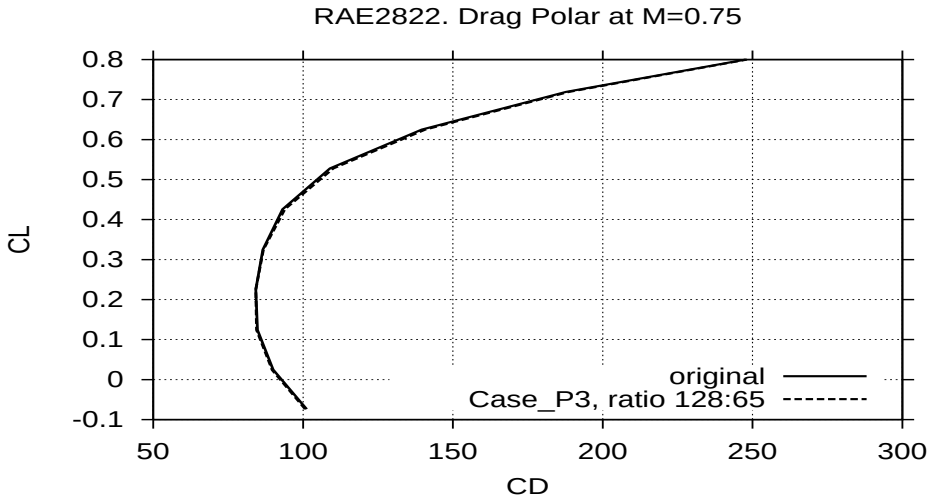

Fig. 8 Drag polar at $M = 0.75$. Case_P3, NPP ratio 128:64 vs. original point-to-point case.